Computers in Biology and Medicine 119 (2020) 103691

Contents lists available at ScienceDirect

Computers in Biology and Medicine

journal homepage: www.elsevier.com/locate/compbiomed

Automated phase classification in cyclic alternating patterns in sleep stages using Wigner–Ville Distribution based features

Shivani Dhok [a], Varad Pimpalkhute [a], Ambarish Chandurkar [a], Ankit A. Bhurane [a,*], Manish Sharma [b], U. Rajendra Acharya [c,d,e]

[a] Department of Electronics and Communication, Indian Institute of Information Technology, Nagpur (IIITN), India
[b] Department of Electrical Engineering, Institute of Infrastructure, Technology, Research and Management (IITRAM), Ahmedabad, India
[c] Department of Electronics and Computer Engineering, Ngee Ann Polytechnic, Singapore 599489, Singapore
[d] Department of Bioinformatics and Medical Engineering, Asia University, Taiwan
[e] International Research Organization for Advanced Science and Technology (IROAST) Kumamoto University, Kumamoto, Japan

ARTICLE INFO

Keywords:
Cyclic alternating patterns (CAP)
Electroencephalogram (EEG)
A-phase
Non rapid eye movements (NREM)
Wigner–Ville Transform
Rényi entropy

ABSTRACT

Sleep is one of the most important body mechanisms responsible for the proper functioning of human body. Cyclic alternating patterns (CAP) play an indispensable role in the analysis of sleep quality and related disorders like nocturnal front lobe epilepsy, insomnia, narcolepsy etc. The traditional manual segregation methods of CAP phases by the medical experts are prone to human fatigue and errors which may lead to inaccurate diagnosis of sleep stages. In this paper, we present an automated approach for the classification of CAP phases (A and B) using Wigner–Ville Distribution (WVD) and Rényi entropy (RE) features. The WVD provides a high-resolution time–frequency analysis of the signals whereas RE provides least time–frequency uncertainty with WVD. The classification is performed using medium Gaussian kernel-based support vector machine with 10-fold cross-validation technique. We have presented the results for randomly sampled balanced data sets. The proposed approach does not require any pre-processing or post-processing stages, making it simple as compared to the existing techniques. The proposed method is able to achieve an average classification accuracy of 72.35% and 87.45% for balanced and unbalanced data sets respectively. The proposed method can aid the medical experts to analyze the cerebral stability as well as the sleep quality of a person.

1. Introduction

Sleep is one of the important elements which is responsible for holistic fitness and proper functioning of the human body. It plays a paramount role in proper functioning as well as in the improvement of the vitality of our body [1]. Studies show that sleep deficiency may cause inability in decision making, problem-solving, controlling the emotions and adaption to rapid changes in people [1,2]. The sleep quality of a person can be quantitatively analyzed using several measures like sleep duration, sleep intensity, sleep continuity and cyclic alternating patterns [2,3]. Sleep is comprised of recurring alternating cycles of rapid eye movement (REM) and non-REM (NREM). In the former class, the person experiences rapid eye movements in all directions. Generally, the REM cycles occur for a short period after the NREM cycles. This repetitive cycle continues. As per the rules presented by Rechtschaffen & Kales in 1968 and the American Academy of Sleep Medicine (AASM) consensus, the sleep is comprised of four stages which include one REM and three NREM stages [4,5]. Several works to classify the sleep stages can be found in literature [6,7]. In 2001, an alternate way for characterization of NREM sleep termed as cyclic alternating pattern (CAP) was proposed [8]. CAP refers to the spontaneous recurrent EEG activity of the non-rapid eye movements (NREM) sleep and is characterized by pseudo-periodic phase-wise transients that alternate with the EEG background pursuits [8]. It represents the instability or disturbance of the sleep. CAP phases play an indispensable role in the analysis of not only sleep disorders but also neurological disorders like insomnia, narcolepsy, etc. Its repetitive pattern assists in the exploration of overall quality of sleep [8].

Each CAP cycle is characterized by two stages, the phase that includes the phasic transients (phase A) and background activities (phase B) [9]. An example of A and B phases in the EEG signals are shown in Fig. 1. The cerebral oscillations of A-phase occur for a duration from 2s to 60 s in NREM stages of the sleep. A-phase is either slow

* Corresponding author.
E-mail addresses: shivanid17499@gmail.com (S. Dhok), pimpalkhutevarad@gmail.com (V. Pimpalkhute), ambarishchdk@gmail.com (A. Chandurkar), ankit.bhurane@gmail.com (A.A. Bhurane), manishsharma.iitb@gmail.com (M. Sharma), aru@np.edu.sg (U. Rajendra Acharya).

https://doi.org/10.1016/j.compbiomed.2020.103691
Received 11 February 2020; Received in revised form 21 February 2020; Accepted 29 February 2020
Available online 4 March 2020

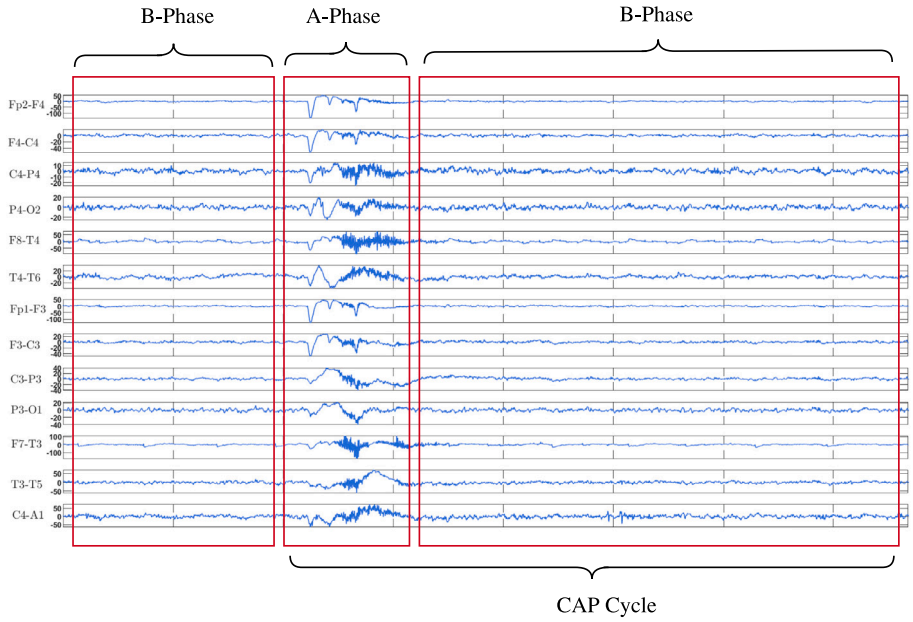

Fig. 1. A and B phases of the CAP cycles (subject name: n5).

varying high amplitude signals or fast varying low amplitude signals or a combination of both. It can be further categorized into three sub-phases, namely A1, A2, and A3. Attempts of sleep preservation are demarcated by A1 phase which occurs in the frequency range of 0.5 Hz to 4 Hz and is designated by delta-bursts and k-complexes [10]. An increase in sleep instability results in high amplitude slow varying signals, leading to A2 and A3 phases. The A3 phase is characterized by alpha and beta waves belonging to the frequency ranges 8 Hz to 12 Hz and 12 Hz to 30 Hz respectively. A2 is a combination of both A1 and A3 phases.

CAP detection not only helps in qualitative analysis of sleep and cerebral surges but also in the diagnosis of diseases like sleep apnea and insomnia [9,11–14]. In practice, the annotation of CAP phases is done by the manual observation by the medical experts, which may lead to human errors and improper classification. This gives rise to the need for automated classification of CAP phases. Many attempts have been made to classify the CAP phases. Most of the developed methods have used the electroencephalogram (EEG) signals. All the major works involve the use of the spectral bands of the EEG signal as well as the onset-offset separation of the CAP phases. The methods developed in the literature not only perform A phase detection but also present A phase classification. One such attempt was presented in [15] where the authors have classified onset-offset of A and B phase using the k-nearest neighbor (KNN) classifier. A similar approach was adopted in [10] in which the onset-offset methodology was used for the separation of A and B phases. The authors have also carried classification of A phase into A1, A2 and A3.

Taking into consideration the existence of CAP phases in specific bands of the EEG signals, many works in the literature have utilized the properties corresponding to various EEG bands for CAP phase segregation. In [16], authors have analyzed six EEG bands (low delta, high delta, theta, alpha, sigma and beta) for feature extraction. They employed A phase detection algorithm using an artificial neural network (ANN). A set of 5 band descriptors in delta, theta, alpha, sigma and beta bands has been used for the recognition of A-Phase and its sub-phases using pre-decided thresholds [17]. The frequency ranges corresponding to the bands are as delta: 0.75–4 Hz, theta: 4–8 Hz, alpha: 8–12 Hz, sigma: 12–15 Hz and beta: 15–25 Hz. The authors in [18] used ANN-based automated NREM isolation followed by segmentation using spectral error measures. A two network cascade approach was presented in [19]. They have employed deep autoencoder for feature extraction and a shallow and optimized ANN for the classification of CAP phases. Another approach of A and B classification and the CAP cycles using finite-state machines (FSM) was presented in [20]. Recently, a temporal analysis method using recurrent neural network (RNN) for classification of CAP phases was introduced in [21]. Apart from neural network techniques, several authors have analyzed the CAP cycles using the basic machine learning (ML) algorithms [10,15,22]. For example, in [22], A-phase segmentation algorithm is illustrated along with ANN, support vector machines (SVM), adaptive boosting and discriminant classifier.

In this paper, we propose the A-phase classification method using Wigner–Ville Distribution (WVD) and Rényi entropy (RE). The Rényi entropy assists in extracting significant information from the time–frequency distributions [23–26]. The reason for utilizing this combo is provision of excellent resolution by WVD in the time–frequency analysis. The Rényi uncertainty is achieved minimum for the WVD, leading to higher information extraction [23]. The main contributions of the paper are as follows.

- Wigner–Ville Distribution (WVD) and RE features are used for the classification of A and B phases of CAP database.
- An overall and subject-wise analysis is performed for six subjects for A-phase detection using balanced data set. The analysis results are compared with unbalanced data set. The uniformity and robustness of the data set is ensured by randomly extracting an equal number of A and B phase samples from each subject. The A-phase samples consist of randomly extracted and balanced sub-phases A1, A2 and A3, thus making this one of the first works of A-phase detection for randomly sampled balanced CAP data set.
- Unlike the existing works, the proposed technique does not require any pre-processing and post-processing stages. Thus simplifying the overall process.

The paper is further organized as follows. The proposed approach and details of data set are given in Section 2. The results presented and discussed in Section 3 and conclusions are drawn in Section 4.

2. Methods and materials

2.1. Data set

We have used the publicly available CAP sleep database [8,27] to develop and evaluate the model. The data set consists of 108

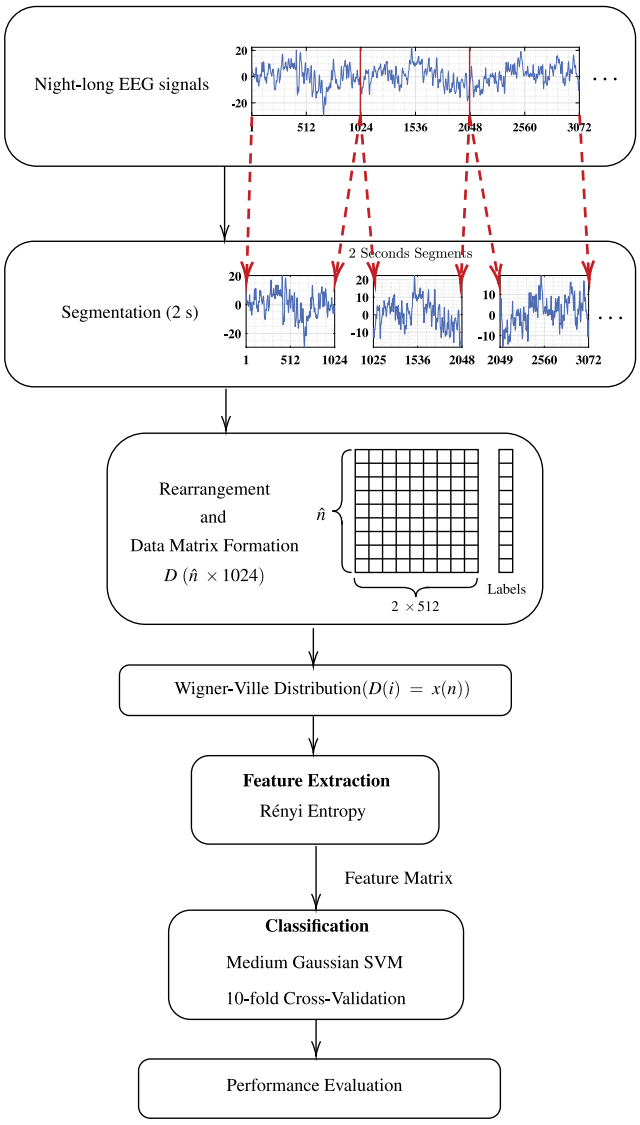

Fig. 2. Work-flow of the proposed method.

polysomnographic recordings registered at Sleep Disorder Center of the Ospedale Maggiore of Parma, Italy [27]. The available data includes at least three EEG channels namely, F3 or F4, C3 or C4 and A1 or A2, two electrooculogram (EOG) channels, submentalis muscle electromyogram (EMG), bilateral anterior EMG, EKG and respiration signals along with some additional traces of bipolar EEG signals. The recordings are categorized as per the subject's pathology like bruxism, insomnia, narcolepsy, nocturnal frontal lobe epilepsy, periodic leg movements, REM behavior disorder, and sleep-disordered breathing. The data was recorded during night and has duration of about 9–10 h. In this work we have used normal (no pathology) data in order to avoid the effects of various pathology disorders.

The data for normal subjects have different sampling rates of 100 Hz, 128 Hz, 200 Hz and 512 Hz. In this work, we have considered data of all 6 subjects that have same sampling frequency of 512 Hz. Other signals with different sampling frequencies can also be considered if resampling is allowed, however, in order to avoid the effects of resampling such signals are not considered. The recordings consist of either C4-A1 or C3-A2 channels of EEG channels. These signals were further segmented in chunks of 2 s Due to insignificance of the CAP phases in the wake (W) state [8], only NREM sleep data has been retained.

Table 1
Total number of samples (unbalanced data set) of A and B phases for six normal condition subjects with a sampling frequency of 512 Hz.

Subject name	Number of samples					
	A1	A2	A3	A (A1+A2+A3)	B	Total (A+B)
n1	1013	354	548	1915	12930	14845
n2	550	327	597	1474	10575	12049
n3	285	284	494	1063	10125	11188
n5	1307	157	377	1841	11475	13316
n10	703	159	445	1307	8550	9857
n11	796	270	386	1452	9225	10677
Total	4654	1551	2847	9052	62880	**71862**

Table 2
Subject-wise data samples obtained after balancing the data set.

Subject name	Number of samples					
	A1	A2	A3	A (A1+A2+A3)	B	Total (A+B)
n1	354	354	354	1062	1062	2124
n2	327	327	327	981	981	1962
n3	284	284	284	852	852	1704
n5	157	157	157	471	471	942
n10	159	159	159	477	477	954
n11	270	270	270	810	810	1620
Total	1551	1551	1551	4653	4653	**9306**

The distribution of total number of samples for the considered 6 subjects are shown in Table 1. It can be observed that the data is highly imbalanced. Hence, for consistency, we adopted an extensive balancing by considering an equal number of samples of A and B phases. The data set consisting of 9306 signals, each of length 1024 is formed. It should be noted that A phase is internally balanced such that an equal number of samples for A1, A2 and A3 sub-phases is considered. The sample selection is done randomly for each subject. Subject-wise number of samples considered for the balanced data set are shown in Table 2.

2.2. Proposed approach

The workflow of the proposed approach is shown in Fig. 2. The NREM segments of the night-long EEG signals are segmented to form a data set that is fed to the feature extraction stage followed by classification.

2.2.1. Wigner–ville distribution

WVD has been recently being used in various biomedical signals classification [28–31]. It is a promising transform which allows us to analyze a signal in high-resolution time–frequency aspects. It has been widely used in the areas of signal visualization, estimation and detection [32–35]. The EEG signals used for the classification of CAP phases lie in different frequency ranges. Hence, time–frequency analysis methods proved to be of a high significance in the analysis of these signals. Typically, for a discrete signal $x(n)$ with N samples, the WVD is given by:

$$X(m,k) = \sum_{n=-N}^{N} \left(x\left(m+\frac{n}{2}\right) x^*\left(m-\frac{n}{2}\right) e^{\frac{-j2\pi kn}{N}} \right), \quad (1)$$

where m and k correspond to the time and frequency components respectively and $j = \sqrt{-1}$. The quantity $x^*(n)$ is the complex conjugate of $x(n)$. For considered case, $x(n)$ is the EEG signal of 2 s duration. The resultant WVD is a 2-D matrix of dimensions $N_f \times 2N$, were N_f is the number of frequency components. For sampling frequency of 512 Hz, the maximum value of frequency correspond to 256 Hz. The significant frequencies for the considered EEG signals range from 0 to 30 Hz with 121 total number of frequency components. Therefore, the dimensions of the WVD matrix is 121 × 2048.

2.2.2. Feature extraction

We have used Rényi entropy (RE) also known as alpha-order entropy, as a feature which is obtained from WVD of EEG data. RE is the generalized form of Shannon entropy and provides more flexibility [36]. The entropy parameters provide us with the degree of randomness in the data. It is calculated by,

$$RE(X_k) = \left(\frac{1}{1-\alpha}\right)\log\left(\sum_{n=1}^{N}|X_k(n)|^{\alpha}\right) \quad (2)$$

where, $N = 2048$ and $(X_k)^{\mathrm{T}}$. Here, $\alpha \neq 1$. For the presented method, Rényi entropy of order 2 is calculated ($\alpha = 2$). So, the equation of RE becomes,

$$RE = -\log\left(\sum_{n=1}^{N}|X_k(n)|^2\right) \quad (3)$$

The RE features result in a feature vector of 121 samples. The extracted feature vectors for each subject are concatenated and labeled to form a feature matrix. The generated feature matrix is fed for classification.

2.3. Classification

The feature matrix obtained at feature extraction stage is further subjected to classification with a 10-fold cross-validation to reduce overfitting [37,38]. We have chosen a medium Gaussian kernel-based support vector machine for classification. Gaussian kernel aids to classify the data with no prior knowledge and also helps to improve the classification of complex data. For our data, Gaussian kernel yielded better separation in higher dimension as compared to other kernels (Refer Table 4). Typically, the classification of data can be achieved depending on the polarity of the hyperplane function and can be given by:

$$H(p) = \sum_{i=1}^{M} w_i K(p, q_i) + b, \quad (4)$$

where w_i, b and q_i are the weights, bias and the support vectors respectively. The kernel function $(K(p, q_i))$ for the Gaussian SVM is defined as [39],

$$K(p, q_i) = \exp\left(-\frac{(p-q_i)^2}{2\sigma^2}\right). \quad (5)$$

2.4. Performance measurement

The various performance parameters used in this work are accuracy, sensitivity, specificity, precision and F1 score [40,41].

3. Results and discussion

The presented approach was implemented on a personal computer equipped with Intel (R) Core (TM) CPU @2.30 GHz 2.30 GHz, 8GB RAM and Windows 10 (64 bit) operating system. The classification was carried out using MATLAB R2019b software, with no other processes running in parallel. The training time and the prediction rate observed for this method is tabulated in Table 3. Medium Gaussian kernel-based SVM classifier was used for the classification. It can be observed from Table 4, that the Gaussian kernel yields higher accuracy as compared to other kernels. Thus making it a better choice for the data under consideration. Moreover, to reduce the over-fitting phenomenon, 10-fold cross-validation was implemented.

The confusion matrix for the balanced data set resulted after the classification process is shown in Fig. 3. The performance parameters evaluated from the confusion matrix are tabulated in Table 5. We have obtained the average accuracy of 72.35% for balanced data set and 87.45% accuracy for the unbalanced data set. The clinical parameters obtained for comparison of balanced and unbalanced data set are shown in Table 6. It can be seen from the table that the specificity and sensitivity values differ significantly for unbalanced and balanced data sets. The receiver operating characteristics [42] for balanced data set is shown in Fig. 4.

The significant RE features were obtained by performing a feature ranking. This was achieved by independent evaluation criterion which

Table 3
Training time and prediction rate using the proposed method for balanced data set with medium Gaussian SVM.

Training time (s)	69.032
Prediction Speed (observations/s)	6000

Table 4
Accuracy values for different kernels of the support vector machine.

Kernel	Accuracy (%)
Linear	70.57
Quadratic	71.26
Cubic	64.52
Gaussian	**72.35**

Table 5
Performance parameters for the balanced data set and Gaussian Kernel.

Performance parameter	Value (%)
Accuracy	72.35
Sensitivity	76.76
Specificity	69.19
Precision	64.11
F1 Score	69.87

Table 6
Comparison of accuracy, specificity and sensitivity using the balanced and unbalanced data set.

Data set	Accuracy (%)	Specificity (%)	Sensitivity (%)
Balanced	72.35 ± 0.20	69.19 ± 0.30	76.76 ± 0.20
Unbalanced	87.45 ± 0.20	52.09 ± 0.10	87.75 ± 0.20

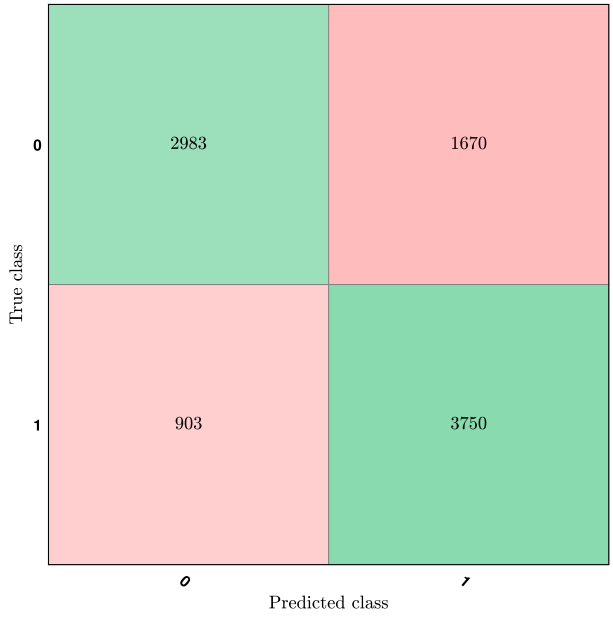

Fig. 3. Confusion matrix for the proposed method using the balanced data set. (Label 0: B-phase, Label 1:A-phase).

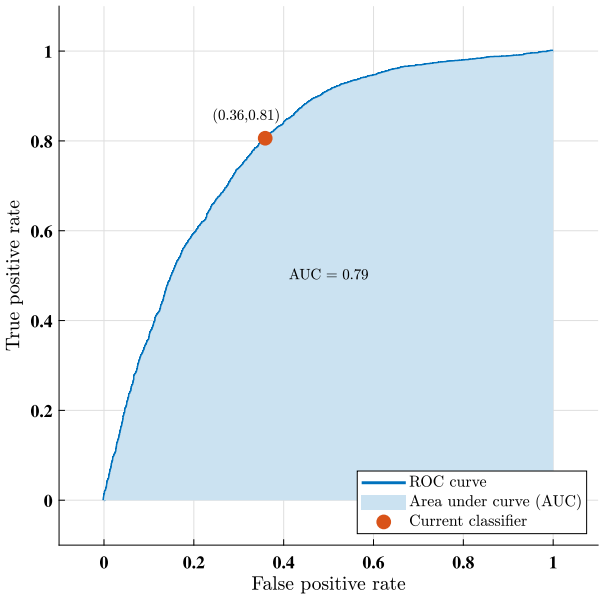

Fig. 4. Receiver operating characteristics for the proposed model using the balanced data set.

Table 7
Summary of cumulative effect of features using the feature ranking with the balanced data set.

Percentage of features	Performance parameters (%)				
	Accuracy	Sensitivity	Specificity	Precision	F1 score
10	68.31	72.77	65.31	58.52	64.87
20	69.01	73.89	65.79	58.80	65.49
30	70.17	74.42	67.18	61.47	67.33
40	71.75	76.45	68.47	62.86	68.99
50	71.87	76.23	68.75	63.55	69.32
60	72.03	76.39	68.90	63.77	69.51
70	72.20	76.38	69.17	64.28	69.81
80	72.28	76.56	69.18	64.22	69.85
90	72.30	76.49	69.25	64.39	69.92
100	72.35	76.76	69.19	64.19	69.87

Table 8
Subject-wise classification results. The data is balanced for each subject (Refer Table 2).

Subject name	Performance parameters (%)				
	Accuracy	Sensitivity	Specificity	Precision	F1 score
n1	78.30	83.20	74.65	70.90	76.56
n2	73.39	77.10	70.58	66.56	71.44
n3	80.46	84.65	77.17	74.41	79.20
n5	78.98	83.05	75.80	72.82	77.60
n10	64.15	63.47	64.90	66.67	65.03
n11	72.59	72.48	72.70	72.84	72.66

operated on sample means hypothesis called Student's t-test criterion [43]. In this method, the features are ranked based on the values of two-sample t-test with pooled variance estimates. The top features are combined based on their ranks and the cumulative performance is tabulated in Table 7. The performance gradually improved with the combination of features. The accuracy versus the top features is plotted in Fig. 5. The increment in accuracy with the number of features can be observed in this figure. Merely 40% of total number of features were able to yield an overall accuracy of >71.8%.

Along with the analysis of combined data for all 6 subjects, we present the subject wise performance. The performance parameters for all the subjects are shown in Table 8. The highest accuracy of 80.46% was obtained for the subject n3. Table 9 shows the comparison of the

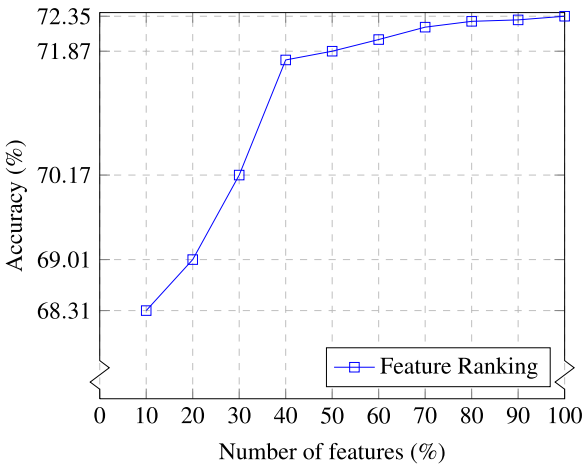

Fig. 5. Accuracy (%) versus number of features obtained using Students' t-test based feature ranking technique for the balanced data set.

results obtained through the proposed method for both balanced and unbalanced data set (refer Table 6). It should be noted that in the previous works the same data set [8,27] has been utilized. It can be seen that the deviation in the values of accuracy, specificity and sensitivity is least by this suggested technique.

4. Conclusions

Cyclic alternating pattern (CAP) assists in effective analysis of sleep quality of a person. It also assists in the analysis of many cerebral disorders like sleep apnea, narcolepsy, etc. In this paper, we present a Wigner–Ville Distribution based feature extraction for the classification of CAP phases using EEG signals. The data set used in this study has been balanced to have equal A-phase and B-phase data samples. The A-phase has internally balanced sub-phases such that each of the sub-phase A1, A2 and A3 have equal data samples. The samples are randomly selected from the subjects. We have used medium Gaussian support vector machine for classification. Moreover, the 10-fold cross-validation technique is used to reduce the overfitting phenomenon. The proposed model is able to achieve the average classification accuracy of 72.35% for balanced data set and 87.45% for unbalanced data set. We have found that, the difference between the specificity and sensitivity are lower for balanced data as compared to the unbalanced data. The clinically significant features are selected using the Student's t-test. It was observed that the combination of features arranged in the decreasing order of their significance improved the classification performance. Apart from the combined analysis, we have also presented a subject-wise analysis. It can be noted from our results that, the deviation in accuracy, specificity and sensitivity is significantly lower as compared to the previously reported methods that used the same CAP sleep database. The proposed algorithm for CAP phase classification is found to be an efficient method which can assist the medical experts in easy analysis of CAP phases, and subsequently diagnose various cerebral problems.

Declaration of competing interest

The authors declare that they have no known competing financial interests or personal relationships that could have appeared to influence the work reported in this paper.

Table 9
Comparison with the state-of-the-art methods for automated phase classification of cyclic alternating patterns of sleep (ACC = Accuracy, SPE = Specificity and SEN = Sensitivity).

Author	Technique	Sampling frequency (Hz)	Number of samples	Performance parameters	Remarks
Mendez et al. [15]	k - Nearest neighbors classifier	100	Unbalanced data A phases: 3963	ACC = 80.00% SPE = 80.00% SEN = 70.00%	KNN based classification wrap approach for feature selection. Pre-processing and post-processing stages involved.
Navona et al. [17]	Recognition based on pre-decided thresholds	128	Unbalanced data	ACC = 77.00% SPE = 90.00% SEN = 84.00%	Pre-processing and post-processing stages involved.
Mariani et al. [18]	ANN classifier along with "EEG segmentation" variable	100	Unbalanced data	ACC = 87.19 ± 2.48% SPE = 90.49 ± 2.80% SEN = 69.55 ± 6.60%	Results mentioned for ANN pre-processing and post-processing steps involved. Large deviation in the values of ACC, SPE and SEN.
Mariani et al. [22]	Machine learning classifiers (SVM, AdaBoost, LDA) and ANN	100	Unbalanced data A-phase: 26305 B-phase: 214,124	ACC = 84.90 ± 4.80% SPE = 86.60 ± 6.30% SEN = 72.50 ± 10.90%	Results mentioned for LDA large deviation in the values of ACC, SPE and SEN
Hartmann et al. [21]	Variable long short-term memory (LSTM) network	128	Both balanced and unbalanced data	ACC = 82.42 ± 6.59% SPE = 83.90 ± 8.95% SEN = 75.28 ± 12.00%	The results are shown for Balanced data using LSTM. Pre-processing and post-processing stages used. Large deviation in the values of ACC, SPE and SEN.
This work	Wigner–Ville based entropy features.	512	Balanced data 9306 (A phase: 4653 B phase: 4653) (A = A1(1551) +A2(1551) +A3(1551)) Unbalanced data 71862	ACC = 72.35 ± 0.20% SPE = 69.19 ± 0.30% SEN = 76.76 ± 0.20% ACC = 87.45 ± 0.20% SPE = 52.09 ± 0.10% SEN = 87.75 ± 0.20%	10-fold cross-validation used no pre-processing or post-processing required. Less deviation in the values of ACC, SPE and SEN.

References

[1] L. National Heart, B. Institute, Sleep deprivation and deficiency, 2019, https://www.nhlbi.nih.gov/health-topics/sleep-deprivation-and-deficiency, (Accessed 1 November 2019).

[2] A.C.M. Liborio Parrino MD, Cyclic alternating pattern, 2014, https://www.medlink.com/index.php/article/cyclic_alternating_pattern, (Accessed 1 November 2019).

[3] WebMD, Sleep disorders, 2019, https://www.webmd.com/sleep-disorders/default.htm, (Accessed 1 November 2019).

[4] A. Kales, A. Rechtschaffen, L.A.B.I.S. University of California, N.N.I.N. (U.S.), A Manual of Standardized Terminology, Techniques and Scoring System for Sleep Stages of Human Subjects: Allan Rechtschaffen and Anthony Kales, Editors, NIH publication, U. S. National Institute of Neurological Diseases and Blindness, Neurological Information Network, 1968, https://books.google.co.in/books?id=wzdRnQEACAAJ.

[5] C. Iber, S. Ancoli-Israel, A. Chesson, S. Quan, The AASM Manual for the Scoring of Sleep and Associated Events: Rules, Terminology and Technical Specifications, American Academy of Sleep Medicine, Westchester, IL, 2007.

[6] M. Sharma, D. Goyal, P. Achuth, U.R. Acharya, An accurate sleep stages classification system using a new class of optimally time-frequency localized three-band wavelet filter bank, Comput. Biol. Med. 98 (2018) 58–75, http://dx.doi.org/10.1016/j.compbiomed.2018.04.025, http://www.sciencedirect.com/science/article/pii/S0010482518301069.

[7] M. Sharma, S. Patel, S. Choudhary, U.R. Acharya, Automated detection of sleep stages using energy-localized orthogonal wavelet filter banks, Arabian J. Sci. Eng. (2019) http://dx.doi.org/10.1007/s13369-019-04197-8.

[8] M.G. Terzano, L. Parrino, A. Sherieri, R. Chervin, S. Chokroverty, C. Guilleminault, M. Hirshkowitz, M. Mahowald, H. Moldofsky, A. Rosa, R. Thomas, A. Walters, Atlas, rules, and recording techniques for the scoring of cyclic alternating pattern (CAP) in human sleep, Sleep Med. 2 (6) (2001) 537–553, http://dx.doi.org/10.1016/S1389-9457(01)00149-6, http://www.sciencedirect.com/science/article/pii/S1389945701001496.

[9] M.G. Terzano, L. Parrino, Clinical applications of cyclic alternating pattern, Physiol. Behav. 54 (4) (1993) 807–813, http://dx.doi.org/10.1016/0031-9384(93)90096-X, http://www.sciencedirect.com/science/article/pii/003193849390096X.

[10] M.O. Mendez, A. Alba, I. Chouvarda, G. Milioli, A. Grassi, M.G. Terzano, L. Parrino, On separability of A-phases during the cyclic alternating pattern, in: 2014 36th Annual International Conference of the IEEE Engineering in Medicine and Biology Society, 2014, pp. 2253–2256, http://dx.doi.org/10.1109/EMBC.2014.6944068.

[11] M. Sharma, M. Raval, U.R. Acharya, A new approach to identify obstructive sleep apnea using an optimal orthogonal wavelet filter bank with ECG signals, Inform. Med. Unlocked (2019) 100170, http://dx.doi.org/10.1016/j.imu.2019.100170, http://www.sciencedirect.com/science/article/pii/S235291481930022X.

[12] M. Sharma, S. Agarwal, U.R. Acharya, Application of an optimal class of antisymmetric wavelet filter banks for obstructive sleep apnea diagnosis using ECG signals, Comput. Biol. Med. 100 (2018) 100–113, http://dx.doi.org/10.1016/j.compbiomed.2018.06.011, http://www.sciencedirect.com/science/article/pii/S0010482518301598.

[13] M. Sharma, P. Achuth, D. Deb, S.D. Puthankattil, U.R. Acharya, An automated diagnosis of depression using three-channel bandwidth-duration localized wavelet filter bank with EEG signals, Cognitive Syst. Res. 52 (2018) 508–520, http://www.sciencedirect.com/science/article/pii/S1389041718302298.

[14] A. Bhurane, S. Dhok, M. Sharma, Y. RAJAMANICKAM, M. M, U.R. Acharya, Diagnosis of parkinson's disease from EEG signals using linear and self-similarity features, Expert Syst. (2019) http://dx.doi.org/10.1111/exsy.12472.

[15] M.O. Mendez, I. Chouvarda, A. Alba, A.M. Bianchi, A. Grassi, E. Arce-Santana, G. Milioli, M.G. Terzano, L. Parrino, Analysis of A-phase transitions during the cyclic alternating pattern under normal sleep, Med. Biol. Eng. Comput. 54 (1) (2016) 133–148, http://dx.doi.org/10.1007/s11517-015-1349-9.

[16] S. Mariani, A.M. Bianchi, E. Manfredini, V. Rosso, M.O. Mendez, L. Parrino, M. Matteucci, A. Grassi, S. Cerutti, M.G. Terzano, Automatic detection of A phases of the Cyclic Alternating Pattern during sleep, in: 2010 Annual International Conference of the IEEE Engineering in Medicine and Biology, 2010, pp. 5085–5088, http://dx.doi.org/10.1109/IEMBS.2010.5626211.

[17] C. Navona, U. Barcaro, E. Bonanni, F. Di Martino, M. Maestri, L. Murri, An automatic method for the recognition and classification of the A-phases of the cyclic alternating pattern, Clinic. Neurophysiol. 113 (11) (2002) 1826–1831, http://dx.doi.org/10.1016/S1388-2457(02)00284-5, https://www.sciencedirect.com/science/article/abs/pii/S1388245702002845.

[18] S. Mariani, A. Grassi, M.O. Mendez, G. Milioli, L. Parrino, M.G. Terzano, A.M. Bianchi, EEG Segmentation for improving automatic CAP detection, Clinic. Neurophysiol. 124 (9) (2013) 1815–1823, http://dx.doi.org/10.1016/j.clinph.2013.04.005, http://www.sciencedirect.com/science/article/pii/S1388245713002654.

[19] S.S. Mostafa, F. Mendonça, A. Ravelo-García, F. Morgado-Dias, Combination of deep and shallow networks for cyclic alternating patterns detection, in: 2018 13th APCA International Conference on Automatic Control and Soft Computing, CONTROLO, 2018, pp. 98–103, http://dx.doi.org/10.1109/CONTROLO.2018.8516418.

[20] F. Mendonça, A. Fred, S.S. Mostafa, F. Morgado-Dias, A.G. Ravelo-García, Automatic detection of cyclic alternating pattern, Neural Comput. Appl. (2018) http://dx.doi.org/10.1007/s00521-018-3474-5.

[21] S. Hartmann, M. Baumert, Automatic a-phase detection of cyclic alternating patterns in sleep using dynamic temporal information, IEEE Trans. Neural Syst. Rehabil. Eng. 27 (9) (2019) 1695–1703, http://dx.doi.org/10.1109/TNSRE.2019.2934828.

[22] S. Mariani, E. Manfredini, V. Rosso, A. Grassi, M.O. Mendez, A. Alba, M. Matteucci, L. Parrino, M.G. Terzano, S. Cerutti, A.M. Bianchi, Efficient automatic classifiers for the detection of a phases of the cyclic alternating pattern in sleep, Med. Biol. Eng. Comput. 50 (4) (2012) 359–372, http://dx.doi.org/10.1007/s11517-012-0881-0.

[23] Tzu-Hsien Sang, W.J. Williams, Renyi information and signal-dependent optimal kernel design, in: 1995 International Conference on Acoustics, Speech, and Signal Processing, vol. 2, 1995, pp. 997–1000, http://dx.doi.org/10.1109/ICASSP.1995.480344.

[24] L. Stankovic, A method for time-frequency analysis, IEEE Trans. Signal Process. 42 (1) (1994) 225–229, http://dx.doi.org/10.1109/78.258146.

[25] W. Williams, M. Brown, A. Hero, Uncertainty, information, and time-frequency distributions, Proc. SPIE 1566 (1991) 144–156, http://dx.doi.org/10.1117/12.49818.

[26] P. Flandrin, R.G. Baraniuk, O. Michel, Time-frequency complexity and information, in: Proceedings of ICASSP '94. IEEE International Conference on Acoustics, Speech and Signal Processing, vol. iii, 1994, pp. III/329–III/332, http://dx.doi.org/10.1109/ICASSP.1994.390031.

[27] A.L. Goldberger, L.A.N. Amaral, L. Glass, J.M. Hausdorff, P.C. Ivanov, R.G. Mark, J.E. Mietus, G.B. Moody, C.-K. Peng, H.E. Stanley, PhysioBank, PhysioToolkit, and PhysioNet, Circulation 101 (23) (2000) e215–e220, http://dx.doi.org/10.1161/01.CIR.101.23.e215.

[28] S.K. Dash, G.S. Rao, Arrhythmia detection using Wigner-Ville distribution based neural network, Procedia Comput. Sci. 85 (2016) 806–811, http://dx.doi.org/10.1016/j.procs.2016.05.269, http://www.sciencedirect.com/science/article/pii/S1877050916306196, International Conference on Computational Modelling and Security (CMS 2016).

[29] S. Sultan Qurraie, R. Ghorbani Afkhami, ECG Arrhythmia classification using time frequency distribution techniques, Biomed. Eng. Lett. 7 (4) (2017) 325–332, http://dx.doi.org/10.1007/s13534-017-0043-2.

[30] R. Abeysekera, B. Boashash, Time-frequency domain features of ECG signals: Their application in P wave detection using the cross Wigner-Ville distribution, vol. 3, 1989, pp. 1524–1527, http://dx.doi.org/10.1109/ICASSP.1989.266731.

[31] R. Pachori, P. Sircar, Time-frequency analysis using time-order representation and Wigner distribution, in: IEEE Region 10 Annual International Conference, Proceedings/TENCON, 2008, pp. 1–6, http://dx.doi.org/10.1109/TENCON.2008.4766782.

[32] R. Sharma, P. Meena, R. Pachori, Enhanced Time-Frequency Representation Based on Variational Mode Decomposition and Wigner-Ville Distribution, 2020.

[33] R. Sharma, A. Kalyani, R. Pachori, An empirical wavelet transform based approach for cross-terms free wigner-ville distribution, Signal Image Video Process. (2019) http://dx.doi.org/10.1007/s11760-019-01549-7.

[34] R. Pachori, A. Nishad, Cross terms reduction in wigner-ville distribution using tunable-q wavelet transform, Signal Process. 120 (2016) 288–304, http://dx.doi.org/10.1016/j.sigpro.2015.07.026.

[35] R. Pachori, P. Sircar, A new technique to reduce cross terms in the wigner distribution, Digit. Signal Process. 17 (2007) 466–474, http://dx.doi.org/10.1016/j.dsp.2006.10.004.

[36] A. Rényi, On measures of entropy and information, in: Proceedings of the Fourth Berkeley Symposium on Mathematical Statistics and Probability, Volume 1: Contributions To the Theory of Statistics, University of California Press, Berkeley, Calif., 1961, pp. 547–561, https://projecteuclid.org/euclid.bsmsp/1200512181.

[37] R. Kohavi, A Study of Cross-Validation and Bootstrap for Accuracy Estimation and Model Selection, Morgan Kaufmann, 1995, pp. 1137–1143.

[38] T. Fushiki, Estimation of prediction error by using K-fold cross-validation, Stat. Comput. 21 (2) (2011) 137–146, http://dx.doi.org/10.1007/s11222-009-9153-8.

[39] V.N. Vapnik, The vicinal risk minimization principle and the SVMs, in: The Nature of Statistical Learning Theory, Springer New York, New York, NY, 2000, pp. 267–290, http://dx.doi.org/10.1007/978-1-4757-3264-1_9.

[40] M. Saito, The precision-recall plot is more informative than the ROC plot when evaluating binary classifiers on imbalanced datasets, PloS One 10 (3) (2015) 1–21, http://dx.doi.org/10.1371/journal.pone.0118432.

[41] C. Goutte, E. Gaussier, A probabilistic interpretation of precision, recall and f-score, with implication for evaluation, in: D.E. Losada, J.M. Fernández-Luna (Eds.), Advances in Information Retrieval, Springer Berlin Heidelberg, Berlin, Heidelberg, 2005, pp. 345–359.

[42] T. Fawcett, An introduction to ROC analysis, Pattern Recognit. Lett. 27 (8) (2006) 861–874, http://dx.doi.org/10.1016/j.patrec.2005.10.010, http://www.sciencedirect.com/science/article/pii/S016786550500303X, ROC Analysis in Pattern Recognition.

[43] Student, The probable error of a mean, Biometrika 6 (1) (1908) 1–25, http://dx.doi.org/10.1093/biomet/6.1.1.